A New Type of Highly Efficient Luminescent Material—The System Al_2O_3−B_2O_3 Containing Ce^{3+} and Tb^{3+} Ions

Hongpeng You,* Guangyan Hong, and Xueyan Wu

Key Laboratory of Rare Earth Chemistry and Physics, Changchun Institute of Applied Chemistry, Chinese Academy of Sciences, Changchun, 130022 People's Republic of China

Jinke Tang and Huiping Hu

Department of Physics, University of New Orleans, New Orleans, Louisiana 70148

Received October 7, 2002. Revised Manuscript Received March 5, 2003

The system Al_2O_3−B_2O_3 containing Ce^{3+} and Tb^{3+} ions was investigated for the first time. It was found that certain compositions give rise to a new highly efficient green luminescent material. The investigation of structure by XRD, ^{11}B MAS NMR spectra, IR spectra, high-resolution electron microscopy, and selected area diffraction images reveals that a crystalline phase and an amorphous phase coexist in the sample. The electron-dispersive X-ray analysis and luminescent studies reveal that the Ce^{3+} and Tb^{3+} ions are doped into the amorphous phase.

Introduction

The luminescence on rare earth ions has been investigated extensively during the past decades, especially on trivalent cerium and terbium ions and on energy transfer between these ions.[1−4] Most of the investigations dealt with the crystalline materials. For example, three commercial green luminescent materials, viz. $Ce_{0.67}Tb_{0.33}MgAl_{11}O_{19}$, (La,Ce,Tb)$PO_4$, and (Gd,Ce,Tb)-$MgB_5O_{10}$, are well-defined crystalline materials. They show high quantum yield and are used in the high-quality tricolor luminescent lamp. On the other hand, luminescence of amorphous materials were paid little attention. This is due to the fact that the quantum yield of an amorphous material[5] is not so high as those of a well-defined crystalline family. However, glasses are well-known in optically pumped laser materials containing Nd^{3+}. To our knowledge, highly efficient crystalline-amorphous materials have not yet been observed. Here, we report a new type of highly efficient green light-emitting material—a crystalline-amorphous material that was discovered in the investigation of the system Al_2O_3−B_2O_3 containing Ce^{3+} and Tb^{3+} ions. The discovery of the new luminescent material may help efforts in design and development of new highly efficient luminescent materials.

The system Al_2O_3−B_2O_3 has already been investigated.[6,7] A tentative phase diagram was given. It shows two compounds, viz. $Al_4B_2O_9$ and $Al_{18}B_4O_{33}$. In the ternary system Al_2O_3−B_2O_3−R_2O_3 (R = Y, Nd, Sm, Eu, Gd, Tb, Dy, Ho, and Yb) only a ternary compound, $RAl_3(BO_3)_4$, was found in the early report.[8,9] Some of them have been used for nonlinear optical material. However, information on the synthesis and the luminescence properties for the system Al_2O_3−B_2O_3 containing Ce^{3+} and Tb^{3+} ions is still lacking. To explore new highly efficient luminescent materials, a series of phosphors in the system Al_2O_3−B_2O_3 containing Ce^{3+} and Tb^{3+} ions with different Al, B, and rare earth ions concentrations was investigated and a new family of luminescent materials was found.

Experimental Section

The starting materials were rare earth oxides (4N), aluminum oxide (4N), and boric acid (GR). Calculated batches were weighed and homogenized in an agate mortar. The mixtures were introduced in an alumina crucible and heated for 2 h at 1250 °C in the presence of carbon.

X-ray powder diffraction measurements were carried out with a Rigaku X-ray diffractometer (model D/max-IIB). The infrared spectrum was measured on a BIO-RAD FTS-7 spectrophotometer. The spectrum was recorded on a KBr pressed disk. The MAS NMR ^{11}B spectra were acquired using a Bruker MSL-400 spectrometer (magnetic field 9.4 T, frequency 128.4 MHz). The zirconia rotors (7 mm in outside diameter) were spun up to 8 kHz; 0.6-μs (π/12) pulses were used with a 0.5-s recycle delay and about 1500 scans accumulated. The chemical shifts are referred to as H_3BO_3. The high-resolution electron microscopy and selected area diffraction images were recorded with a transmission electron microscope (model JEOL-2010) with EDAX DX Prime electron-dispersive X-ray analysis (EDS). The excitation and emission spectra were recorded on an Hitachi F-4500 fluorescence spectrofluorimeter at room

* To whom correspondence should be addressed. E-mail: hpyou@ns.ciac.jl.cn.

(1) Blasse, G. *Chem. Mater.* **1989**, *1*, 294.
(2) Yocom, P. N. *J. SID* **1996**, *4/3*, 149.
(3) Yocom, P. N.; Meltzer, R. S.; Jang, R. W.; Grimm, M. *J. SID* **1996**, *4/3*, 169.
(4) Jütel, T.; Nikol, H.; Ronda, C. *Angew. Chem., Int. Ed.* **1998**, *37*, 3084.
(5) Verwey, J. W. M.; Blasse, G. *Mater. Chem. Phys.* **1990**, *25*, 91.
(6) Scholze, H. *Z. Anorg. Allg. Chem.* **1956**, *284*, 272.
(7) Gielsse, P. J. M.; Foster, W. R. *Nature* **1962**, *195*, 69.
(8) Ballman, A. A. *Am. Mineral* **1962**, *47*, 1380.
(9) Mills, A. D. *Inorg. Chem.* **1962**, *1*, 960.

10.1021/cm0209923 CCC: $25.00
Published on Web 04/12/2003

Table 1. Value of Brightness of $8.4Al_2O_3 \cdot xB_2O_3 \cdot 0.35Ce_2O_3 \cdot 0.25Tb_2O_3$ under 254-nm Excitation (Compared with Commercial Magnesium Aluminate)

phosphors	brightness
(Ce,Tb) $MgAl_{11}O_{19}$	100
$8.4Al_2O_3 \cdot 3B_2O_3 \cdot 0.35Ce_2O_3 \cdot 0.25Tb_2O_3$	38
$8.4Al_2O_3 \cdot 4B_2O_3 \cdot 0.35Ce_2O_3 \cdot 0.25Tb_2O_3$	96
$8.4Al_2O_3 \cdot 5B_2O_3 \cdot 0.35Ce_2O_3 \cdot 0.25Tb_2O_3$	103
$8.4Al_2O_3 \cdot 6B_2O_3 \cdot 0.35Ce_2O_3 \cdot 0.25Tb_2O_3$	102
$8.4Al_2O_3 \cdot 7B_2O_3 \cdot 0.35Ce_2O_3 \cdot 0.25Tb_2O_3$	95

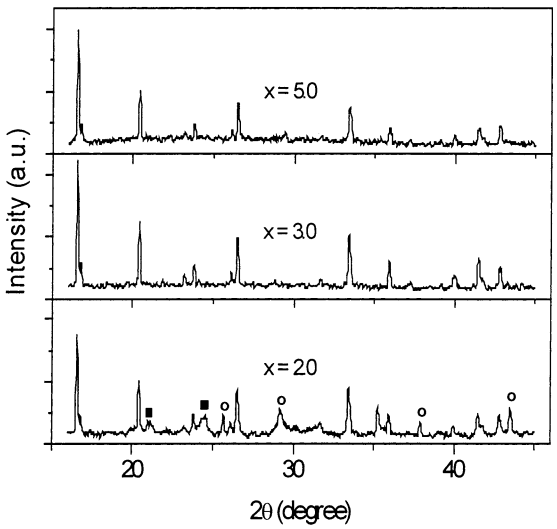

Figure 1. XRD spectra of $8.4Al_2O_3 \cdot xB_2O_3 \cdot 0.35Ce_2O_3 \cdot 0.25Tb_2O_3$.

temperature. The excitation spectra were corrected for the lamp output. The emission spectra were corrected for the photo-multiplier sensitivity.

Results and Discussion

Table 1 shows the brightness of the samples with proper Al, B, and rare earth ions concentrations. It reveals that a new highly efficient green luminescent material can be obtained at certain conditions in the $Al_2O_3-B_2O_3$ system containing Ce^{3+} and Tb^{3+} ions.

To explore the structure of the samples, the X-ray diffraction (XRD) spectra of the sample were investigated (Figure 1). The spectrum of the sample with $x = 2.0$ shows that there are strong diffraction peaks of $Al_{18}B_4O_{33}$ phase along with weak diffraction peaks of Al_2O_3 and unidentified crystalline phases that may be associated with the rare earth ions, indicating that $Al_{18}B_4O_{33}$ is the predominant phase in the sample.

As x varies from 2.0 to 3.0, the diffraction peaks of Al_2O_3 and unidentified crystalline phases disappear. Only $Al_{18}B_4O_{33}$ phase is observed. On the increase of the x value from 3.0 to 5.0, the intensity of the diffraction peaks of $Al_{18}B_4O_{33}$ phase slightly decreases and no new diffraction peak is observed. This result reveals that a change in structure occurs with an increase in the B_2O_3 concentration.

From the XRD results mentioned above, it seems that rare earth ions are doped into the $Al_{18}B_4O_{33}$ phase on increasing B concentration. Due to larger radii of rare earth ions, it is impossible that rare earth ions directly replace Al^{3+} or B^{3+}. On the other hand, it is difficult to identify an amorphous phase by XRD when a crystalline phase and an amorphous phase coexist. Therefore, it can be inferred that there are two possibilities: one is

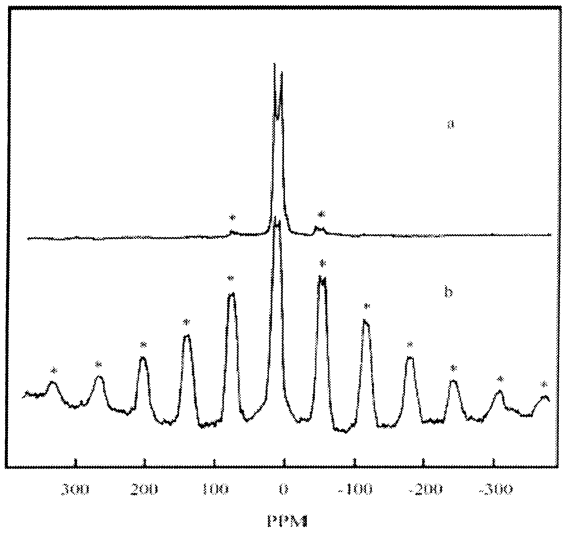

Figure 2. ^{11}B MAS NMR spectra of $Al_{18}B_4O_{33}$ (a) and $8.4Al_2O_3 \cdot 5B_2O_3 \cdot 0.35Ce_2O_3 \cdot 0.25Tb_2O_3$ (b).

that the increase of B_2O_3 concentration leads to the substitution of Al^{3+} ions by B^{3+} and rare earth ions in view of the compensation of the radii, which means that B^{3+} replaces the Al^{3+} of AlO_4 to meet the needs of the coordination number of B^{3+} and the structure of the $Al_{18}B_4O_{33}$.[10] The other is that the increase in the B^{3+} concentration may give rise to the formation of an amorphous phase, and rare earth ions are doped into an amorphous phase. These inferences will be discussed below.

Figure 2 shows the ^{11}B MAS NMR spectrum of $Al_{18}B_4O_{33}$ and $8.4Al_2O_3 \cdot 5B_2O_3 \cdot 0.35Ce_2O_3 \cdot 0.25Tb_2O_3$. The spectrum of $Al_{18}B_4O_{33}$ shows a strong band at about 10 ppm and a very weak band at about 1 ppm. Previous investigations[11-13] on the B-containing compounds have shown that the ^{11}B MAS NMR spectrum can readily distinguish BO_3 from BO_4 units. The signal with isotropic chemical shifts for BO_4 units is in the region from 2 to -10 ppm, while the signal for BO_3 units is from 5 to 32 ppm. Therefore, the strong band is due to BO_3 units, and the very weak band at about 1 ppm is due to BO_4 units, which indicates that B^{3+} is mainly in the form of BO_3 units and is consistent with the literature.[10] Due to second-order quadrupole interactions, the band of ^{11}B of BO_3 units is broadened and split. The spectrum also contains spinning sidebands, which are identified by varying the spinning speed of the sample whereupon they change position while the central resonance remains fixed.

As for $8.4Al_2O_3 \cdot 5B_2O_3 \cdot 0.35Ce_2O_3 \cdot 0.25Tb_2O_3$, the ^{11}B MAS NMR spectrum shows a band from 6 to 18 ppm and strong spinning sidebands. The band from 6 to 18 ppm is also attributed to BO_3 units. The strong spinning sidebands are related to the presence of stronger magnetic materials compared with $Al_{18}B_4O_{33}$. For example, the spinning sidebands of ^{27}Al in aluminosili-

(10) Ihara, M.; Imai, K.; Fukunaga, J.; et al. *Kogyo Kyokaishi* **1980**, *88* (2), 77.
(11) Turner, G.; Smith, K. A.; Kirkpatrick, R. J.; Oldfeld, E. *J. Magn. Reson.* **1986**, *67*, 544.
(12) Richard, K. B.; David, R. T.; Gary, L. *J. Am. Ceram. Soc.* **1997**, *80*, 1239.
(13) Chadeyron, G.; El-Ghozzi, M.; Mahiou, R.; Arbus, A.; Cousseims, J. C. *J. Solid State Chem.* **1997**, *128*, 261.

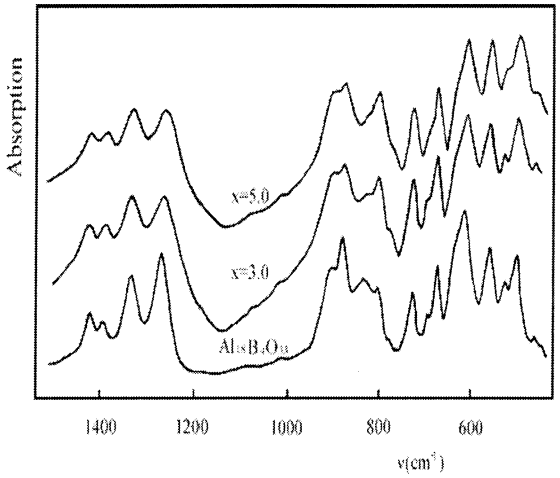

Figure 3. IR spectra of $8.4Al_2O_3{\cdot}xB_2O_3{\cdot}0.35Ce_2O_3{\cdot}0.25Tb_2O_3$ and $Al_{18}B_4O_{33}$.

cates[14] are strongly increased when ferromagnetic oxide is doped. So is the case for $8.4Al_2O_3{\cdot}5B_2O_3{\cdot}0.35Ce_2O_3{\cdot}0.25Tb_2O_3$. In fact, Ce^{3+} and Tb^{3+} ions are paramagnetic ions, while Al^{3+}, B^{3+}, and O^{2-} are diamagnetic ions. The extensive spinning sideband formation is in good agreement with the fact that the presence of paramagnetic Ce^{3+} and Tb^{3+} ions in the sample leads to stronger magnetism of the sample than that of $Al_{18}B_4O_{33}$.

Figure 3 shows the IR spectra of $8.4Al_2O_3{\cdot}xB_2O_3{\cdot}0.35Ce_2O_3{\cdot}0.25Tb_2O_3$ and $Al_{18}B_4O_{33}$. The spectrum of $Al_{18}B_4O_{33}$ is very complex and more than a cursory interpretation is not possible. However, it is generally accepted[15−19] that the vibration absorption in region 1200−1460 cm^{-1} is due to B−O bond asymmetric stretching of BO_3 units, while that in the range 1000−1100 cm^{-1} originates from B−O bond asymmetric stretching of BO_4 units. Therefore, the bands appearing in the 1500−1200-cm^{-1} region are due to B−O bond asymmetric stretching of BO_3 units. Very weak bands observed in the region 1000−1100 cm^{-1} are assigned to the B−O bond asymmetric stretching of BO_4 units.

Relative to the spectrum of pure $Al_{18}B_4O_{33}$, three major changes associated with the increasing B-concentration containing Ce^{3+} and Tb^{3+} ions are observed. First, the bands corresponding to $Al_{18}B_4O_{33}$ become weak with increasing B-content, indicating that the amount of $Al_{18}B_4O_{33}$ phase is decreased. Second, the background intensity in different regions increases with increasing B-concentration. The background in the region from 1500 to 1200 cm^{-1} is due to the broad band absorption, originating from new BO_3 units. Third, the absorption at about 803 cm^{-1}, which is assigned to out-of-plane deformation vibrations of BO_3 units, clearly increases in intensity with increasing B-concentration. These spectra changes suggest that there exists another phase.

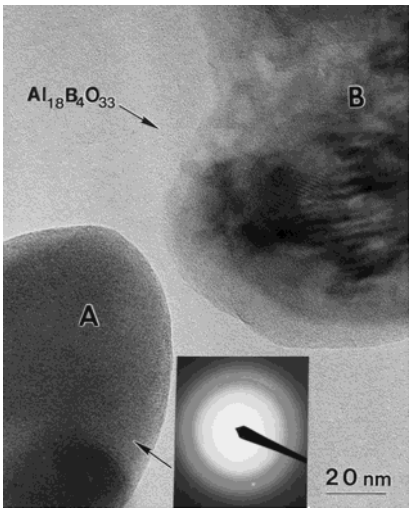

Figure 4. High-resolution electron microscopy and selected area diffraction image of $8.4Al_2O_3{\cdot}xB_2O_3{\cdot}0.35Ce_2O_3{\cdot}0.25Tb_2O_3$.

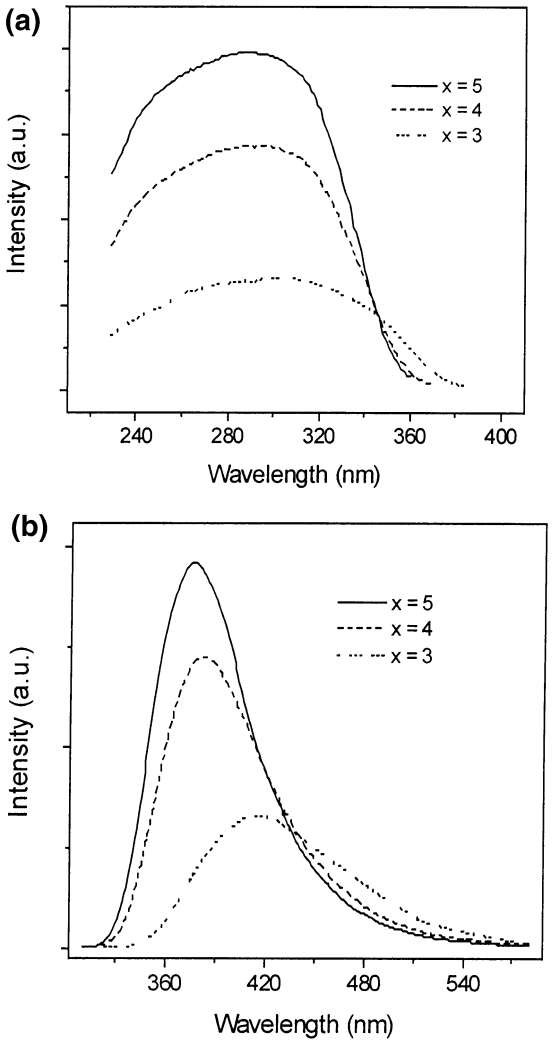

Figure 5. (a) Excitation spectra of $8.65Al_2O_3{\cdot}xB_2O_3{\cdot}0.35Ce_2O_3$. ($x = 5.0$, $\lambda_{em} = 375$ nm; $x = 4.0$, $\lambda_{em} = 384$ nm; $x = 3.0$, $\lambda_{em} = 416$ nm). (b) Emission spectra of $8.65Al_2O_3{\cdot}xB_2O_3{\cdot}0.35Ce_2O_3$. ($x = 5.0$, $\lambda_{ex} = 288$ nm; $x = 4.0$, $\lambda_{ex} = 292$ nm; $x = 3.0$, $\lambda_{ex} = 304$ nm).

The IR spectrum changes mentioned above, along with the results of XRD, suggest that there is an amorphous phase. Considering the fact that there is no definite change in the BO_4 units in the sample in terms

(14) Oldfield, E.; Kinsey, R. A.; Smith, K. A.; Nichols, J. A.; Kirkpatrick, R. J. *J. Magn. Reson.* **1983**, *51*, 325.
(15) Kamitsos, E. I.; Kiarakassides, M. A.; Chryssikos, G. D. *J. Phys. Chem.* **1987**, *91*, 1073.
(16) Rulmont, A.; Almou, M. *Spectrochim. Acta, Part A* **1989**, *45*, 603.
(17) Hilic, S.; Zambon, D.; Chadeyron, G.; et al. *J. Alloy Compd.* **1998**, *275*, 301.
(18) Lemanceau, S.; Bertrand-chadeyron, G.; Mahion, R.; El-Ghozzi, M.; Cousseins, J. C. *J. Solid State Chem.* **1999**, *148*, 229.
(19) Wang, G.; Wu, Y.; Fu, X.; Liang, X.; Xu, Z.; Chen, C. *Chem. Mater.* **2002**, *14*, 2044.

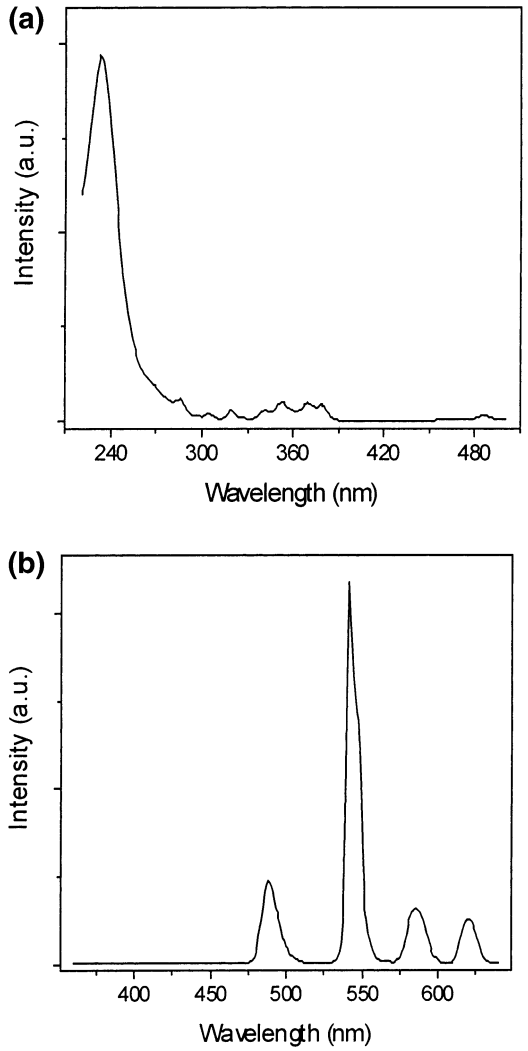

Figure 6. (a) Excitation spectrum of $8.75Al_2O_3 \cdot 5B_2O_3 \cdot 0.25Tb_2O_3$ ($\lambda_{ex} = 541$ nm). (b) Emission spectrum of $8.75Al_2O_3 \cdot 5B_2O_3 \cdot 0.25Tb_2O_3$ ($\lambda_{em} = 233$ nm).

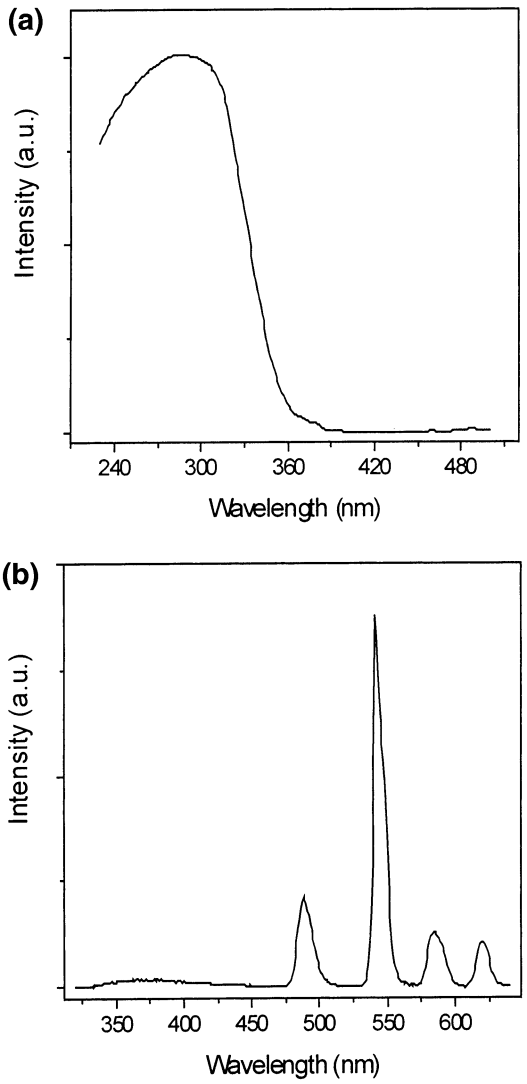

Figure 7. (a) Excitation spectrum of $8.4Al_2O_3 \cdot 5B_2O_3 \cdot 0.35Ce_2O_3 \cdot 0.25Tb_2O_3$. ($\lambda_{em} = 541$ nm). (b) Emission spectrum of $8.4Al_2O_3 \cdot 5B_2O_3 \cdot 0.35Ce_2O_3 \cdot 0.25Tb_2O_3$. ($\lambda_{ex} = 288$ nm).

of the results on the ^{11}B MAS NMR spectra and IR spectra, it is impossible that Al^{3+} is substituted by B^{3+} and the rare earth ions. Therefore, it is strongly suggested that rare earth ions are doped into an amorphous phase with increasing B-concentration. This conclusion is confirmed by direct electron diffraction observation.

Figure 4 shows the high-resolution electron microscopy (HREM) and selected area diffraction (SAD) images. It shows that there are two types of particles A and B. Particle A has the disorder structure and diffuse rings, while particle B shows fringes of lattice planes. This is a direct indication that amorphous phase and crystalline phase coexist in the sample. It should be noted that there are weak diffraction rings in the amorphous particle A, indicating that a small amount of crystallites still exist. Furthermore, we have applied EDAX and electron diffraction techniques to identify crystalline $Al_{18}B_4O_{33}$ in particle B. At the same time, we have also identified elements B, O, Al, Ce, and Tb in amorphous particle A and element B, O, and Al in crystalline particle B. Thus, it is quite clear that crystalline phase and amorphous phase coexist in the sample and rare earth ions are doped into the amorphous phase.

Parts a and b of Figure 5 show the excitation and emission spectra of $8.65Al_2O_3 \cdot xB_2O_3 \cdot 0.35Ce_2O_3$. Both excitation and emission spectra show a broad band, corresponding to the allowed 4f−5d transitions of the Ce^{3+} ions. One property of the emission spectra is the absence of the doublet arising from the spin−orbit splitting of the $4f^1$ ground state ($^2F_{5/2}$ and $^2F_{7/2}$) of Ce^{3+} ions. Another is that the position of Ce^{3+} ion emission band changes with the x value. These characteristic features of Ce^{3+} emission spectra are quite similar to that of Ce^{3+} in amorphous phases. In fact, the Ce^{3+} emission band in amorphous phases have two striking characteristic features:[5,20] one is that the spin−orbit splitting of the Ce^{3+} ground state ($^2F_{7/2}$ and $^2F_{5/2}$) cannot be resolved, due to the inhomogeneous broadening; the other is that the position of the Ce^{3+} emission band changes with the composition of the matrix. Thus, the luminescent properties of the Ce^{3+} ions reveal a variation of Ce surroundings and indicate that the Ce^{3+} ions are doped into the amorphous phase.

(20) Chao, Z. J.; Parent, C.; Le Flem, G.; Hagenmuller, P. *J. Solid State Chem.* **1991**, *93*,17.

With increasing x value, the excitation and emission bands shift to higher energy, implying that the extent of covalence of the Ce^{3+} ions may be lower, that is, have higher ionicity. There are more borate groups that surround the Ce^{3+} ion in a direction away from the central Ce^{3+} ion, viz. on the side opposite to the Ce^{3+} ion,[1] in accordance with the increase of B_2O_3 concentration. The Stokes shift of the Ce^{3+} emission in the composition $x = 5.0$ is $\sim$8056 cm^{-1} and is 8856 cm^{-1} at $x = 3.0$. The smaller Stokes shift shows a more stiff coordination around the Ce^{3+} ions in the composition with $x = 5.0$. The decrease in the Stokes shift is responsible for the higher intensity of Ce^{3+} luminescence in composition $x = 5$. Therefore, B concentration plays a crucial role in the formation of efficient luminescent centers. Moreover, the position of the Ce^{3+} emission band changes with B concentration in the region of the Tb^{3+} strong f−f absorption. This may lead to a highly efficient energy transfer between Ce^{3+} and Tb^{3+} ions if the Ce^{3+} emission peak matches well with stronger f−f absorption of Tb^{3+} ions. This point will be described below.

Parts a and b of Figure 6 show the excitation and emission spectra of $8.75Al_2O_3 \cdot 5B_2O_3 \cdot 0.25Tb_2O_3$. The excitation is composed of sharp bands in the region from 280 to 500 nm and a broad band peaking at about 233 nm. The broad band is ascribed to the spin-allowed transition from 4f to 5d of Tb^{3+} ion. The sharp bands correspond to absorption of the forbidden f−f transitions. The stronger absorptions of f−f transition are located at about 352, 370, and 380 nm. The emission spectrum under 254-nm excitation consists of four bands located at about 489, 541, 589, and 622 nm. The four bands are due to the $^5D_4 \rightarrow {}^7F_J$ ($J = 6$, 5, 4, and 3) transitions, respectively. These emission bands show inhomogeneous broadening characteristics, revealing that Tb^{3+} ions were doped into amorphous phase. Moreover, the emission from the $^5D_3$ level of Tb^{3+} has not been observed in this sample, which is expected. This observation may be explained by the quenching of the efficient multiphonon de-excited with lattice vibration due to the high energy of phonons in the borates.

Parts a and b of Figure 7 show the excitation and emission spectra of $8.4Al_2O_3 \cdot 5B_2O_3 \cdot 0.35Ce_2O_3 \cdot 0.25Tb_2O_3$. The excitation spectrum of the sample monitored at 541 nm consists mainly of Ce^{3+} excitation bands and very weak Tb^{3+} absorption bands, indicating that Tb^{3+} is essentially excited through Ce^{3+} ions. In fact, several weak f−f absorption bands of Tb^{3+} ions are just in the region of the Ce^{3+} emission. Thus, energy transfer from Ce^{3+} to Tb^{3+} occurs. The emission spectrum of the sample contains both very weak emission of Ce^{3+} and strong green emission of the Tb^{3+}, indicating that the Ce^{3+}−Tb^{3+} energy transfer is highly efficient. This result is due to the fact that the emission peak of Ce^{3+} ions in this host matches well with the stronger f−f absorption of the Tb^{3+} ions.

In summary, the experimental results described here have shown for the first time that certain compositions in the Al_2O_3−B_2O_3 system containing Ce^{3+} and Tb^{3+} ions give a new type of highly efficient green luminescent material via high-efficiency energy transfer between Ce^{3+} and Tb^{3+}. It has been demonstrated that the new green luminescent material is a crystalline-amorphous material.

Acknowledgment. This work was financially supported by the National Science Foundation of China (Grant No. 20071031.).

CM0209923